Research Article | Vol. 25, No. 1 | 9 Jan 2017 | OPTICS EXPRESS 431

Optics EXPRESS

Enhanced optical magnetism for reversed optical binding forces between silicon nanoparticles in the visible region

TAKA-AKI YANO,[1,2,*] YUTA TSUCHIMOTO,[1] REMO PROIETTI ZACCARIA,[3] ANDREA TOMA,[3] ALEJANDRO PORTELA,[1] AND MASAHIKO HARA[1,2,4]

[1]*School of Materials and Chemical Technology, Tokyo Institute of Technology, Yokohama, Kanagawa, 226-8502, Japan*
[2]*RIKEN, 2-1 Hirosawa, Wako, Saitama 351-0198, Japan*
[3]*Istituto Italiano di Tecnologia, Via Morego 30, 16163 Genova, Italy*
[4]*Earth-Life Science Institute, Tokyo Institute of Technology, Meguro, Tokyo 152-8551, Japan*
[*]*yano@echem.titech.ac.jp*

Abstract: We perform a comprehensive numerical analysis on the optical binding forces of a multiple-resonant silicon nanodimer induced by the normal illumination of a plane wave in the visible region. The silicon nanodimer provides either repulsive or attractive forces in water while providing only attractive forces in air. The enhancement of the magnetic dipole mode is attributed to the generation of repulsive forces. The sign (attractive/repulsive) and the amplitude of the optical forces are controlled by incident polarization and separation distance between the silicon nanoparticles. These optomechanical effects demonstrate a key step toward the optical sorting and assembly of silicon nanoparticles.

OCIS codes: (290.0290) Scattering; (310.6628) Subwavelength structures, nanostructures; (350.4855) Optical tweezers or optical manipulation.

References and links

1. R. W. Bowman and M. J. Padgett, "Optical trapping and binding," Rep. Prog. Phys. **76**(2), 026401 (2013).
2. K. Dholakia and P. Zemanek, "Colloquium: Gripped by light: Optical binding," Rev. Mod. Phys. **82**(2), 1767–1791 (2010).
3. E. Lamothe, G. Lévêque, and O. J. F. Martin, "Optical forces in coupled plasmonic nanosystems: Near field and far field interaction regimes," Opt. Express **15**(15), 9631–9644 (2007).
4. B. Sepúlveda, J. Alegret, and M. Käll, "Nanometric control of the distance between plasmonic nanoparticles using optical forces," Opt. Express **15**(22), 14914–14920 (2007).
5. Q. Zhang, J. J. Xiao, X. M. Zhang, Y. Yao, and H. Liu, "Reversal of optical binding force by Fano resonance in plasmonic nanorod heterodimer," Opt. Express **21**(5), 6601–6608 (2013).
6. L. Huang and O. J. F. Martin, "Reversal of the optical force in a plasmonic trap," Opt. Lett. **33**(24), 3001–3003 (2008).
7. A. S. Zelenina, R. Quidant, and M. Nieto-Vesperinas, "Enhanced optical forces between coupled resonant metal nanoparticles," Opt. Lett. **32**(9), 1156–1158 (2007).
8. M. Nieto-Vesperinas, R. Gomez-Medina, and J. J. Saenz, "Angle-suppressed scattering and optical forces on submicrometer dielectric particles," J. Opt. Soc. Am. A **28**(1), 54–60 (2011).
9. E. Xifré-Pérez, F. J. García de Abajo, R. Fenollosa, and F. Meseguer, "Photonic binding in silicon-colloid microcavities," Phys. Rev. Lett. **103**(10), 103902 (2009).
10. A. I. Kuznetsov, A. E. Miroshnichenko, Y. H. Fu, J. Zhang, and B. Luk'yanchuk, "Magnetic light," Sci. Rep. **2**, 492 (2012).
11. Y. H. Fu, A. I. Kuznetsov, A. E. Miroshnichenko, Y. F. Yu, and B. Luk'yanchuk, "Directional visible light scattering by silicon nanoparticles," Nat. Commun. **4**, 1527 (2013).
12. A. B. Evlyukhin, S. M. Novikov, U. Zywietz, R. L. Eriksen, C. Reinhardt, S. I. Bozhevolnyi, and B. N. Chichkov, "Demonstration of magnetic dipole resonances of dielectric nanospheres in the visible region," Nano Lett. **12**(7), 3749–3755 (2012).
13. R. Regmi, J. Berthelot, P. M. Winkler, M. Mivelle, J. Proust, F. Bedu, I. Ozerov, T. Begou, J. Lumeau, H. Rigneault, M. F. García-Parajó, S. Bidault, J. Wenger, and N. Bonod, "All-dielectric silicon nanogap antennas to enhance the fluorescence of single molecules," Nano Lett. **16**(8), 5143–5151 (2016).
14. M. Caldarola, P. Albella, E. Cortés, M. Rahmani, T. Roschuk, G. Grinblat, R. F. Oulton, A. V. Bragas, and S. A. Maier, "Non-plasmonic nanoantennas for surface enhanced spectroscopies with ultra-low heat conversion," Nat. Commun. **6**, 7915 (2015).

#280579 http://dx.doi.org/10.1364/OE.25.000431
Journal © 2017 Received 10 Nov 2016; revised 27 Dec 2016; accepted 28 Dec 2016; published 6 Jan 2017

Optics EXPRESS

15. T. Wu, X. H. Zhang, R. Y. Wang, and X. D. Zhang, "Strongly enhanced Raman optical activity in molecules by magnetic response of nanoparticles," J. Phys. Chem. C **120**(27), 14795–14804 (2016).
16. A. E. Krasnok, A. E. Miroshnichenko, P. A. Belov, and Y. S. Kivshar, "All-dielectric optical nanoantennas," Opt. Express **20**(18), 20599–20604 (2012).
17. I. Staude, A. E. Miroshnichenko, M. Decker, N. T. Fofang, S. Liu, E. Gonzales, J. Dominguez, T. S. Luk, D. N. Neshev, I. Brener, and Y. Kivshar, "Tailoring directional scattering through magnetic and electric resonances in subwavelength silicon nanodisks," ACS Nano **7**(9), 7824–7832 (2013).
18. B. Rolly, B. Stout, and N. Bonod, "Boosting the directivity of optical antennas with magnetic and electric dipolar resonant particles," Opt. Express **20**(18), 20376–20386 (2012).
19. S. Person, M. Jain, Z. Lapin, J. J. Sáenz, G. Wicks, and L. Novotny, "Demonstration of zero optical backscattering from single nanoparticles," Nano Lett. **13**(4), 1806–1809 (2013).
20. Y. Tsuchimoto, T. A. Yano, T. Hayashi, and M. Hara, "Fano resonant all-dielectric core/shell nanoparticles with ultrahigh scattering directionality in the visible region," Opt. Express **24**(13), 14451–14462 (2016).
21. U. Zywietz, M. K. Schmidt, A. B. Evlyukhin, C. Reinhardt, J. Aizpurua, and B. N. Chichkov, "Electromagnetic resonances of silicon nanoparticle dimers in the visible," ACS Photonics **2**(7), 913–920 (2015).
22. P. Albella, M. A. Poyli, M. K. Schmidt, S. A. Maier, F. Moreno, J. J. Saenz, and J. Aizpurua, "Low-loss electric and magnetic field-enhanced spectroscopy with subwavelength silicon dimers," J. Phys. Chem. C **117**(26), 13573–13584 (2013).
23. J. Yan, P. Liu, Z. Lin, H. Wang, H. Chen, C. Wang, and G. Yang, "Directional Fano resonance in a silicon nanosphere dimer," ACS Nano **9**(3), 2968–2980 (2015).
24. B. Rolly, B. Bebey, S. Bidault, B. Stout, and N. Bonod, "Promoting magnetic dipolar transition in trivalent lanthanide ions with lossless Mie resonances," Phys. Rev. B **85**(24), 245432 (2012).
25. E. D. Palik, *Handbook of Optical Constants of Solids* (Academic, 1985).
26. D. J. Griffiths, *Introduction to Electrodynamics* (Prentice Hall, 1999).

1. Introduction

Optical binding has recently been recognized as a fascinating phenomenon in the field of optical trapping for the highly precise control of multiple nanoparticles in aqueous environments [1, 2]. It is driven by interparticle forces mediated by light without special shaping of the light field, as opposed to ordinary optical trapping, which relies on gradient and scattering forces. Optical binding forces have been studied well for pairs of microparticles and have recently been investigated intensively for pairs of plasmonic nanostructures [3–7]. The optical binding forces exerted between resonant plasmonic nanostructures can be attractive or repulsive depending on the separation distance, the incident polarization, and the excitation wavelength.

In addition to plasmonic materials, dielectric materials with high indices of refraction and low energy losses have recently been regarded as promising resonant scatterers to generate strong optical binding forces [8,9]. Among the high index materials, silicon (Si) nanoparticles with diameters of 100–200 nm have gained much attention owing to their multiple electromagnetic resonances in the visible region [10–12], which have been recently utilized for field-enhanced spectroscopies [13–15]. Electric dipoles (EDs) and magnetic dipoles (MDs) excited in the Si nanoparticles lead to novel scattering properties enabling unidirectional scattering and even zero-backscattering arising from the interference of EDs and MDs inside the particles [11, 16–20]. More interestingly, when two Si nanoparticles are in close proximity to each other, the EDs and MDs of the particles mutually interact [21–24], resulting in an enhancement of the electric and magnetic fields and directional Fano resonance depending on the separation distance.

In this study, inspired by the multiple resonances of a Si nanodimer at optical frequencies in the near-field regime, we perform a comprehensive numerical study of the optical binding forces on a single Si nanodimer in water to achieve practical applications for the optical sorting and assembling of multiple Si nanoparticles. This study addresses a crucial difference in the optical binding forces between Si nanodimers and plasmonic gold nanodimers. For plane wave illumination parallel to the dimer axis, the Si nanodimers exhibit repulsive or attractive binding forces, whereas the plasmonic nanodimers exhibit only an attractive component over the entire visible region. The central mechanism of the repulsion for the Si nanodimer is discussed based on the interplay between the EDs and MDs of the Si nanodimers.

Optics EXPRESS

2. Results and discussion

For the numerical analysis, a finite element method software package, COMSOL (COMSOL Inc., Burlington, MA, USA), was used to solve Maxwell's equations for a nanodimer consisting of a pair of Si nanoparticles with a variable interparticle separation. The diameter of each Si nanoparticle in the dimer was set to 100–160 nm so that the ED and MD modes could co-exist in the visible wavelength region. A plane wave with an intensity of 1 W/μm^2 was incident in the direction perpendicular to the dimer axis. The dielectric constant (ε) of crystalline Si was obtained from experimental data by Palik (for example, $\varepsilon = 16.6 + 0.26i$ at ~550 nm and $\varepsilon = 15.5 + 0.19i$ at ~600 nm) [25]. On the basis of the simulated full-wave electromagnetic field solutions, the optical binding force exerted on a nanoparticle in the longitudinal direction (i.e., the dimer axis) was calculated numerically using the Maxwell stress tensor method. The resulting optical binding force is negative for attraction (bonding) and positive for repulsion (anti-bonding).

Figures 1(a) and 1(b) show the calculated scattering cross-section and the optical binding force between the Si nanoparticles in air and water, respectively. Two Si nanoparticles with the same diameter of 160 nm were separated from each other by 5 nm and illuminated by a plane wave polarized along the dimer axis, as shown in the insets of Figs. 1(a) and 1(b). In air, multiple peaks originating from the ED and MD resonances are observed in the scattering spectrum. The optical force is always attractive over the entire visible region and reaches a maximum at approximately 650 nm, which is slightly offset from the strongest resonant wavelength in the scattering spectrum. In water, however, the optical force becomes a repulsive force at wavelengths of ~480 nm and ~600 nm and an attractive force in other wavelength regions [Fig. 1(b)]. Before starting a detailed discussion of the reversed optical binding force of the Si nanodimer in water, it is informative to compare the optical force of the Si nanodimer with that of a gold nanodimer. In air, a gold nanodimer consisting of two gold nanoparticles with the same diameter of 100 nm and the gap distance of 5 nm possesses the lowest-order longitudinal modes of the dimer that originate from the coupled ED oscillations in the visible region and result in an attractive optical force maximized exactly at the resonant wavelength. When the gold nanodimer is placed in water, as shown in Fig. 1(d), the resonant wavelength is red-shifted by approximately 100 nm and corresponds to the wavelength at which the maximum attractive force is induced. However, unlike the Si nanodimer in Fig. 1(b), the gold nanodimer in water does not produce the repulsive portion of the optical binding force. Rather, the attractive force increases as the surrounding refractive index increases from 1.0 to 1.33 because of the increasing ED-induced field enhancement at the separation gap in water. This result implies that the presence of the MD resonance, excited for the Si nanodimer but not for the gold nanodimer in this wavelength region, has a crucial contribution to the repulsive optical force of the Si dimer in water.

It should be noted that the attractive van der Waals force (vdW) between the water-immersed Si nanoparticle is around 180 pN, the absolute value of which is comparable to that of the optically-induced repulsive force at 600 nm in Fig. 1(b). Considering that the optical force is proportional to the excitation power, further increase in the excitation power would overwhelm the effect of the attractive vdW.

Optics EXPRESS

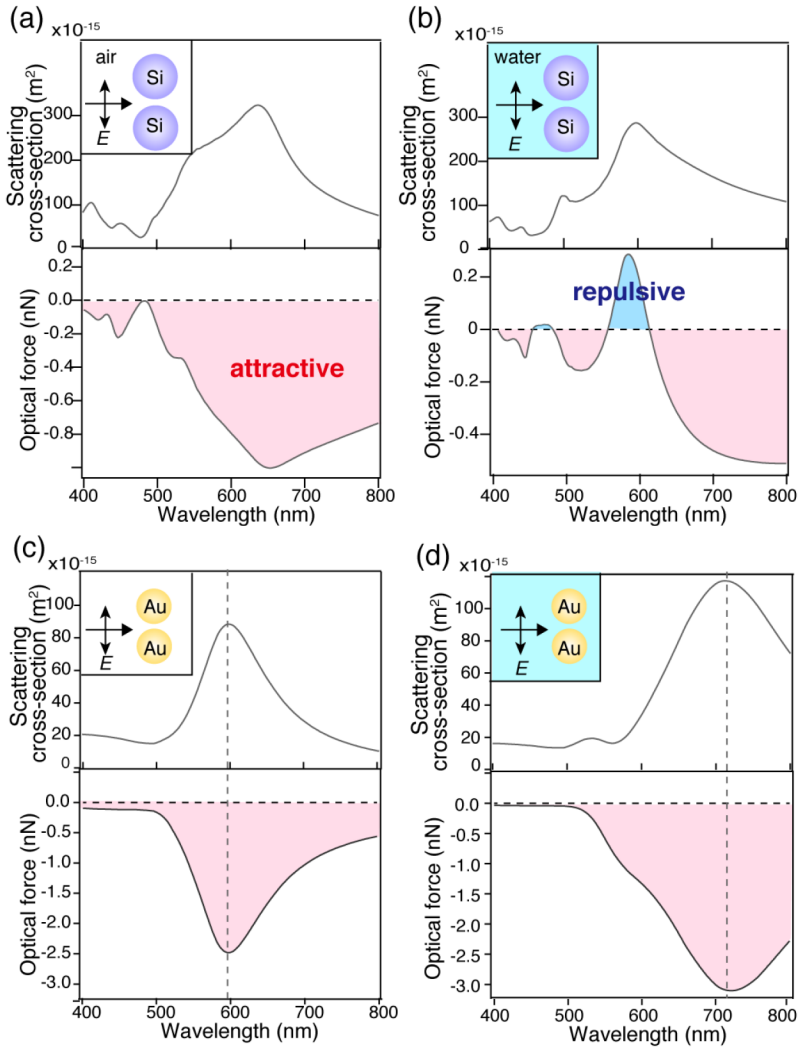

Fig. 1. Scattering cross-sections and optical binding forces of a Si nanodimer with a diameter of 160 nm in (a) air and (b) water for incident light polarized parallel to the dimer axis. The same data set for a gold nanodimer with a diameter of 100 nm in (c) air and (d) water. The interparticle separation of each dimer is 5 nm. The intensity of the incident light is 1 W/μm^2 for all cases.

To reveal the underlying mechanism of the repulsive optical force in water, it is instructive to decompose the complex multiple resonances into the ED and MD components of the Si nanodimer. As reported previously [21, 22], when Si nanoparticles of a dimer are placed in close proximity, the ED and MD moments excited in each Si nanoparticle mutually interact, resulting in hybrid ED and MD modes. On the basis of the well-established dipole–dipole model [21, 22], we calculated the hybrid ED and MD modes of our Si nanodimer. Given that the ambient surrounding medium (air) in our model is replaced by water in Fig. 1, the ED and MD spectra were obtained with a gradually increasing surrounding refractive index (n_0) from 1.0 (air) to 1.33 (water), which are shown in Figs. 2(a) and 2(b), respectively. The ED spectra are characterized by a broad peak ranging over nearly the entire visible region. As the refractive index increases, the ED mode shifts to the longer wavelength region in association with a decrease in its intensity. This decrease in the intensity is due to the fact that the ED becomes small in association with the decrease in the index contrast between the

Optics EXPRESS

spheres and the surrounding medium. Conversely, the MD spectrum for n_0 = 1.0 exhibits two hybridized peaks appearing at 540 nm and 640 nm [see the black line in Fig. 2(b)]. Those peaks can be effectively regarded as the following two modes: the latter one is a pure MD mode which is directly excited by an incident light, the former one is known as an indirect ED mode where a directly excited MD induces a ED in another sphere through a near-field interaction [21, 22]. Here the energy for exciting MDs is distributed in these two different modes. When increasing n_0 to 1.33, the indirect ED mode exhibits a pronounced red-shift and a significant increase in its intensity. This increase in the intensity is attributed to the enhancement of the near-field interaction because electric fields penetrating from the spheres into the surrounding medium are gained by the low index contrast. On the other hand, the pure MD mode exhibits a rapid decrease in its intensity. This is because a lot of the energy for exciting MDs is distributed in the indirect ED mode due to the strong near-field interaction. Interestingly, the refractive index-dependent resonant wavelengths of the shorter MD component are in close association with those of the characteristic peaks indicated by the arrows in the optical force spectra of Fig. 2(c), indicating the primary contribution of the shorter MD component to the repulsive nature of the optical force.

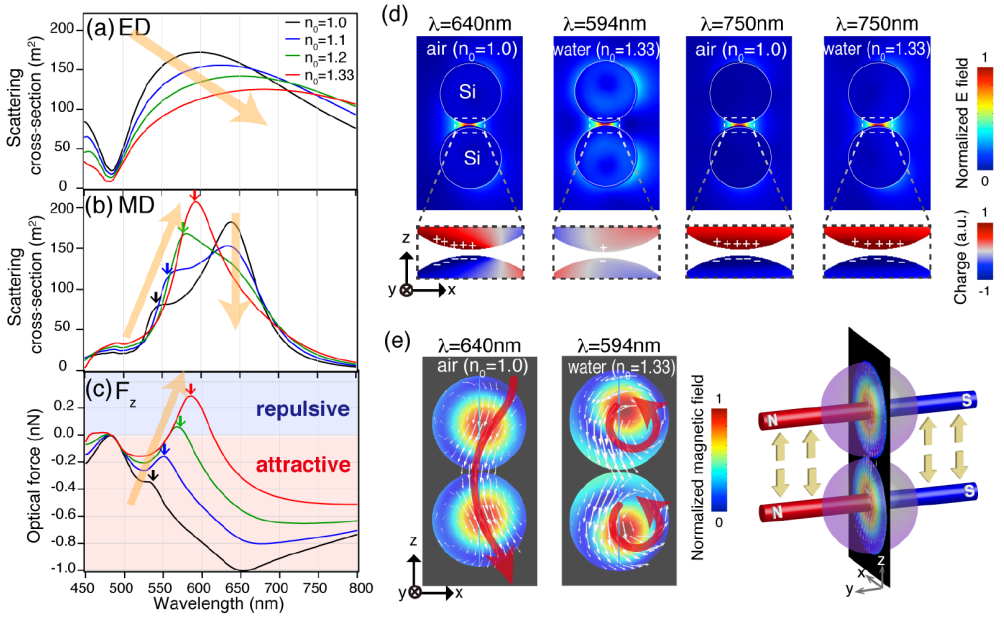

Fig. 2. Scattering spectra of the (a) ED and (b) MD modes and the (c) optical binding force of the Si nanodimer calculated while increasing the surrounding refractive index (n_0) from 1.0 to 1.33. (d) Electric field distribution (top) and surface charge density (bottom) at 640 nm (n_0 = 1.0), 594 nm (n_0 = 1.33), 750 nm (n_0 = 1.0), and 750 nm (n_0 = 1.33). (e) Magnetic field distribution along with the current flow indicated by white arrows at 640 nm (n_0 = 1.0) and 594 nm (n_0 = 1.33). The right side of panel (e) schematically shows that the repulsive force is generated at 594 nm (n_0 = 1.33) owing to the magnetic Lorentz force.

To further examine the contribution of the hybrid ED and MD modes to the net optical binding force, the electric near-field distributions were calculated for each dipolar resonance. The two left panels in Fig. 2(d) show the calculated electric near-field distributions around the Si dimer at the strongest MD resonant wavelengths of 640 nm for n_0 = 1.0 and 594 nm for n_0 = 1.33, whereas the two right panels show the distributions at 750 nm where the dimer is still in the ED resonance but out of the MD resonance for n_0 = 1.0 and n_0 = 1.33. The incident field is strongly localized at the separation gap of the dimer for all the wavelengths because of the resonant excitation of the broad ED. However, inside each Si nanoparticle of the dimer,

Optics EXPRESS

the MD-like field distribution is visible only at the MD resonant wavelength (594 nm) for n_0 = 1.33, owing to the suppression of the ED resonance at n_0 = 1.33.

It is also worth examining the surface charge density (bottom panels in Fig. 2(d)) of the dimer in the vicinity of the gap in order to investigate the Coulomb interaction between the two Si nanoparticles. In general, the Si dimer itself is not as completely conductive as plasmonic metals; therefore, the charges can be distributed not only on the surface but also inside the dimer. However, as shown in the near-field distributions in Fig. 2(d), the electric field is dominantly localized at the gap of the dimer because of the high index nature of Si, enabling treatment of only the surface charges when considering the Coulomb interaction. As shown in Fig. 2(d), the opposite charges are localized on either side of the dimer gap at all resonant wavelengths, resulting in the generation of an attractive force between the nanoparticles. However, the charge density for the MD resonance at 594 nm in water is much lower than that for the other resonances because of the smaller field confinement and enhancement at the gap, resulting in a smaller attractive interaction, as indicated in Fig. 2(c).

To directly discuss the contribution of the MD resonance to the repulsive force, the magnetic field distributions at the strongest MD resonant wavelengths, both for n_0 = 1.0 and n_0 = 1.33, are shown in Fig. 2(e) along with the current flow indicated by the white arrows. In both cases, MDs are clearly generated in each nanoparticle of the dimer in the same direction as the y-axis; therefore, we expect a circular current flow around each MD. However, in the case of n_0 = 1.0, the mainstream current flow, as schematically indicated by the red arrow, is from one particle to the other across the gap and not localized and circulating around each particle. This is because the densely localized charges near the gap dominate the flow crossing the gap and prevent the current from flowing around the individual MDs; therefore, the attractive force dominates in air at the MD resonant wavelength. Conversely, in water (n_0 = 1.33), the current can primarily flow circularly around the MD in each particle owing to the much lower charge density in the proximity of the gap compared with that in air. As schematically shown in the right side of Fig. 2(e), the circularly flowing current generates artificial magnetic fields close to each other in the same direction, generating a Lorentz force caused by the magnetic repulsion. This is why a repulsive force is generated between the nanoparticles at the MD resonant wavelength in water, as shown in Fig. 1(b).

The dependence of the separation distance of the Si nanodimer in water on the optical binding force was also numerically investigated. Figure 3(a) shows the calculated optical binding forces for different separation distances ranging from 2 nm to 50 nm. The nanodimer was immersed in water and illuminated by a plane wave polarized along the dimer axis, as schematically shown in the inset of Fig. 3(a). The corresponding scattering spectra, decomposed into the MD and ED components by the analytical dipole–dipole model, are shown in Figs. 3(b) and 3(c), respectively. The origin of the repulsion in Fig. 3(a) is explicable in the same manner as that in Fig. 2(e), that is, via the interaction between the optically induced MDs in each Si nanoparticle at the MD resonant wavelength. Consequently, the peak positions of the repulsive portion for different distances in Fig. 3(a) correspond to the MD resonant wavelengths in Fig. 3(b). In general, when two dipoles with the same magnetic moments are aligned in parallel with separation distance d, the repulsive force originating from the dipole–dipole interaction is known to decrease with the fourth power of d [26]. However, Fig. 3(a) shows that the peak intensity of the repulsive portion gradually increased as the separation distance increased. This is because the peak intensities of the MD resonances in Fig. 3(b) increase with distance, contributing to the increase in the MD-induced magnetic repulsive force. In addition, the suppression of the Coulombic attractive force, originating from the decrease in the ED resonance with distance at wavelengths longer than 580 nm in Fig. 3(c), further highlights the contribution of the repulsive force to the net binding force as the distance increases.

Inspired by the distance-dependent spectroscopic natures of the optical binding force, we plotted the optical binding forces in Fig. 3(d) as a function of the distance for two different

Optics EXPRESS

wavelengths of 580 nm and 620 nm, which correspond to the MD resonant wavelengths for the separation distances of 2 nm and 50 nm, respectively. As the distance decreases from 50 nm to 10 nm, the optical force at 580 nm gradually increases in the repulsive region and then decreases when the distance is further decreased. Conversely, the force at 620 nm gradually decreases with decreasing distance and finally becomes attractive at the proximal distance. This result suggests a promising technique for the sorting of Si nanoparticles by properly selecting the excitation wavelength.

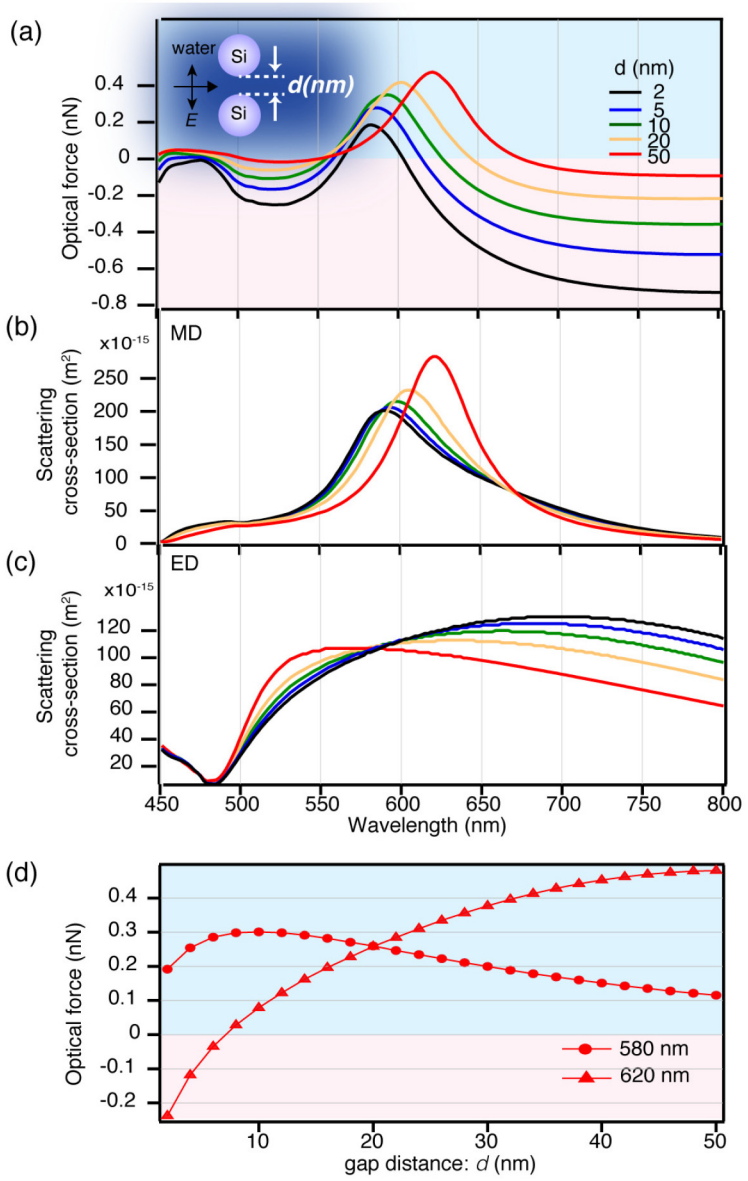

Fig. 3. (a) Optical binding force and the scattering cross-section of the (b) MD and (c) ED modes of the Si nanodimer calculated with increasing separation distance (*d*) from 2 to 50 nm. (d) Distance-dependent optical binding force at 580 nm and 620 nm.

Optics EXPRESS

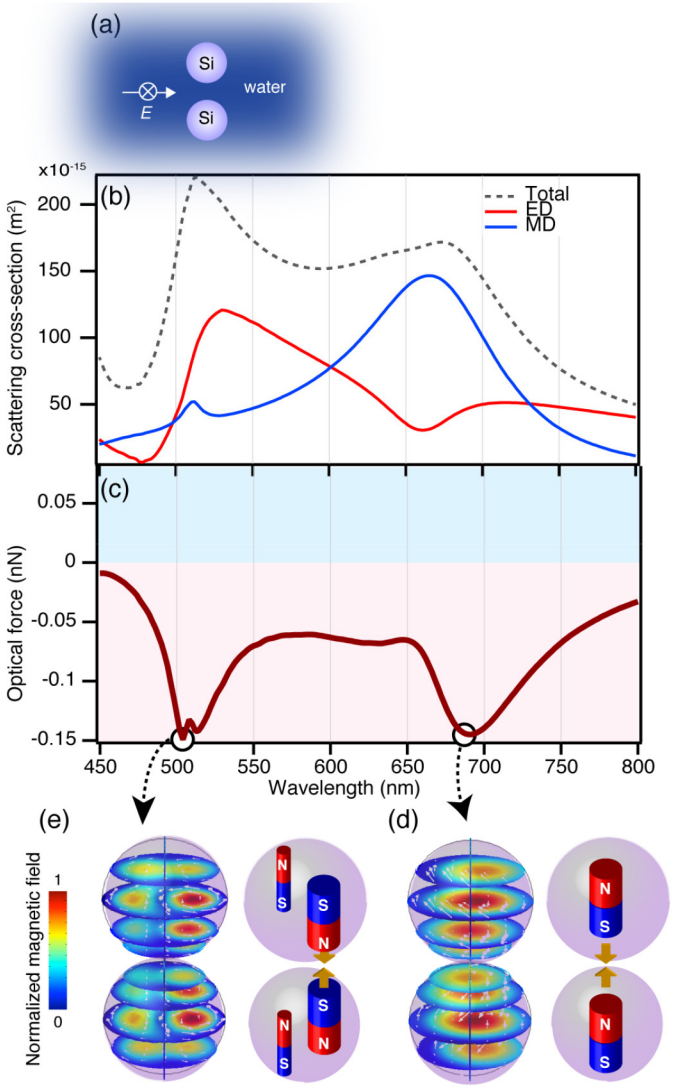

Fig. 4. (a) Schematic of a Si nanodimer with a diameter of 160 nm in water for incident light polarized perpendicular to the dimer axis. (b) Scattering cross-section and (c) optical binding force of the Si nanodimer. The magnetic field distribution with a comprehensive schematic of the artificially induced magnetic force at (d) 680 nm and (e) 500 nm.

Finally, the optical force of the Si nanodimer in water under illumination with the incident polarization perpendicular to the dimer axis [see the schematics in Fig. 4(a)] was comprehensively numerically investigated. Figure 4(b) shows the total scattering spectrum along with the decomposed ED and MD components. The corresponding optical force of the nanodimer in Fig. 4(c) shows three distinct dips in the attractive region at 500 nm, 520 nm, and 680 nm. In the case of perpendicular polarization, the electric field induced by the ED is localized at the side surface of each particle (see Fig. S1), whereas in the case of parallel polarization, it is localized in the vicinity of the separation gap, as shown in Fig. 2. Therefore, the ED resonance for the perpendicular polarization does not induce the Coulombic attractive force observed in Fig. 2. Consequently, we considered the contribution of the MD resonances to the attractive force components (three dips) in Fig. 4(c). Interestingly, we found that the positions of the dips in the attractive region at 520 nm and 680 nm correspond to the peak

Optics EXPRESS

positions of the MD resonances in Fig. 4(b). Figure 4(d) shows the magnetic field distribution inside each Si nanoparticle at one of the MD resonances (680 nm). Strong magnetic fields in each Si nanoparticle are induced in the same direction along the dimer axis, artificially mimicking two magnets with the North (N) and South (S) poles stacking in line, as schematically shown in the right side of Fig. 4(d). The opposite poles face each other in the vicinity of the separation gap, resulting in an attractive binding force at the MD resonant wavelength. The origin of the remaining dip at 500 nm observed in Fig. 4(c) can also be explained via the corresponding magnetic field distribution. As shown in Fig. 4(e), the magnetic field distribution corresponds to magnetic quadrupoles excited in each Si nanoparticle even though the magnetic field is distributed inhomogeneously along the incident direction. The schematic in the right side of Fig. 4(e) shows that the magnetic quadrupoles mimic the two magnets in each Si nanoparticle, inducing a strong attractive binding force along the dimer axis. Therefore, the strong attractive force components observed for the perpendicular polarization can be attributed to optically induced attractive magnetism, originating from magnetic dipole–dipole and quadrupole–quadrupole interactions.

3. Summary

In summary, we comprehensively addressed the critical roles of magnetic resonances in achieving the reversed optical binding force of the Si nanodimer in water at optical frequencies. The optically induced magnetic force was observed to be controllable via the refractive index of the surrounding medium, the incident polarization, the incident wavelength, and the separation distance between two Si nanoparticles. These fundamental studies on the optically induced artificial magnetism of the Si nanodimer provide a promising platform for optically controlled sorting and self-assembling of multiple Si nanoparticles.

Funding

Japan Society for the Promotion of Science (JSPS) Grant-in-Aid for scientific research (26706006).

Acknowledgment

This work was partially supported by JSPS Core-to-Core Program, A. Advanced Research Networks.